HHS Public Access

Author manuscript

Kidney Int. Author manuscript; available in PMC 2017 March 01.

Published in final edited form as:

Kidney Int. 2016 March ; 89(3): 612–624. doi:10.1016/j.kint.2015.11.017.

Uroplakin 1b is critical in urinary tract development and urothelial differentiation and homeostasis

Ashley R. Carpenter, BS[1,2], **Brian Becknell, MD, PhD**[2], **Christina B. Ching, MD**[2], **Edward J. Cuaresma, JD**[3], **Xi Chen, PhD**[1], **David S. Hains, MD**[4], and **Kirk M. McHugh, PhD**[1,5]

[1]Molecular and Human Genetics, Nationwide Children's Hospital

[2]College of Medicine, Ohio State University

[3]Urology, Nationwide Children's Hospital

[4]Children's Foundation Research Institute at Le Bonheur Children's Hospital, University of Tennessee Health Science Center

[5]Division of Anatomy, Ohio State University.

Abstract

Proper development and maintenance of urothelium is critical to its function. Uroplakins are expressed in developing and mature urothelium where they establish plaques associated with the permeability barrier. Their precise functional role in development and disease is unknown. Here, we disrupted *Upk1b in vivo* where its loss resulted in urothelial plaque disruption in the bladder and kidney. *Upk1bRFP/RFP* bladder urothelium appeared dysplastic with expansion of the progenitor cell markers, Krt14 and Krt5, increased Shh expression, and loss of terminal differentiation markers Krt20 and uroplakins. *Upk1bRFP/RFP* renal urothelium became stratified with altered cellular composition. *Upk1bRFP/RFP* mice developed age-dependent progressive hydronephrosis. Interestingly, 16% of *Upk1bRFP/RFP* mice possessed unilateral duplex kidneys. Our study expands the role of uroplakins, mechanistically links plaque formation to urinary tract development and function, and provides a tantalizing connection between congenital anomalies of the kidney and urinary tract along with functional deficits observed in a variety of urinary tract diseases. Thus, kidney and bladder urothelium are regionally distinct and remain highly plastic, capable of expansion through tissue-specific progenitor populations. Furthermore, *Upk1b* plays a previously unknown role in early kidney development representing a novel genetic target for congenital anomalies of the kidney and urinary tract.

Address correspondence to: Ashley R. Carpenter, Research Institute at Nationwide Children's Hospital, Columbus, OH 43205, USA. F | (614) 722-2817 P | (614) 355-2879 | ashley.carpenter@nationwidechildrens.org.

DISCLOSURE

None to disclose

Keywords

bladder; CAKUT; development; kidney; uroplakins; urothelium

INTRODUCTION

Urothelium is a specialized epithelium that lines the urinary tract. Although contiguous, the morphology and developmental ontology of urothelium are tissue-specific.[1] Most studies focus on multi-layered bladder urothelium, limiting our understanding of urothelium in the remaining urinary tract.

Normal urothelial function is critical in maintaining the urine:blood barrier, modulating surface area, and mediating the host response to infection.[2, 3] Evidence points to a role for urothelium in patterning of the urinary tract.[4, 5] Furthermore, studies in our lab and others have shown molecular and structural alterations in renal urothelium to be an early response to tissue injury.[6-8]

Critical to urothelial function is formation of an apical asymmetrical unit membrane (AUM). AUM plaques are composed of uroplakin (Upk) protein particles.[3, 9] Five have been identified: Upk1a, Upk1b, Upk2, Upk3a and Upk3b.[9-13] Upk1a and Upk1b are tetraspanin proteins and possess four transmembrane (TM) domains, whereas, Upk2 and Upk3 have single TM domains.[3]

Upks are assembled in the endoplasmic reticulum (ER; **Figure 1.1**), where they heterodimerize prior to escaping the ER (**Figure 1.2**). Upk1a and Upk1b heterodimerize with Upk2 and Upk3, respectively. Further processing in the Golgi apparatus leads to a conformational change and heterotetramer formation (**Figure 1.3**). Upk heterotetramers form concentric hexameric rings (**Figure 1.4**) of highly organized Upk particles that are packaged into vesicles and trafficked to the cell surface.[9, 14-16] Rigid urothelial plaques are a hallmark of urothelial differentiation and are highly conserved among mammals.[9, 17]

We investigated the function of *Upk1b* in bladder and kidney urothelium. *In vivo* manipulation of a tetraspanin Upk has never been evaluated. Our results indicate that the urothelial plaque is critical to urothelial development, homeostasis and function and that *Upk1b* represents a new genetic target for congenital anomalies of the kidney and urinary tract (CAKUT).

RESULTS

Bladder

Upk1b-directed RFP expression was validated in $Upk1b^{RFP/+}$ and $Upk1b^{RFP/RFP}$ urinary tracts (**Supplemental Figure 1A-C**). As expected, *Upk1b* mRNA expression was decreased in a stepwise manner from high levels in controls to low levels in $Upk1b^{RFP/RFP}$ bladders (**Supplemental Figure 1D**). This negatively correlated with graded increases in RFP expression in $Upk1b^{RFP/+}$ and $Upk1b^{RFP/RFP}$ bladders (**Supplemental Figure 1E**).

Altered morphology and absent plaque

Upk1b ablation resulted in dysplastic urothelial morphology with anisokaryosis and abnormal nuclear alignment (**Supplemental Figure 1H**). Round vacuoles with apoptotic cells, and narrow, clear, pericellular spaces, consistent with cellular retraction were observed. Histopathology is summarized (**Tables 1 & 2**).

Urothelial plaque appeared absent in *Upk1b*$^{RFP/RFP}$ bladders (**Figure 2A, B**) and was confirmed by scanning electron microscopy (**Supplemental Figure 2**). The apical surface had fewer and more blunted microvillar projections with surface cells exhibiting immature vesicles and a reduced number and density of ribosomes. Urothelial plaque components were significantly affected by *Upk1b* ablation (**Figure 2 C-L**). Upk3a, Upk3b and Upk2 protein expression was reduced in *Upk1b*$^{RFP/RFP}$ bladders, although *Upk3a* and *Upk2* mRNA appeared unchanged and *Upk3b* increased slightly. Upk3a appeared absent from *Upk1b*$^{RFP/RFP}$ bladder urothelium, while Upk3b, Upk2 and Upk1a were significantly reduced and/or aberrantly localized.

Altered cellular composition and increased proliferation

Urothelial organization was significantly altered in *Upk1b*$^{RFP/RFP}$ bladders (**Figure 3**). Umbrella cell marker, Krt20, exhibited increased mRNA expression in *Upk1b*$^{RFP/RFP}$ bladders, while protein levels appeared reduced (**Figure 3A-E**). Intermediate cell marker, Krt13, was expanded throughout the urothelium with intense staining in the apical layer, which normally does not express Krt13 (**Figure 3A, F, G**).

Basal cell markers, Krt5 and Krt14, were altered in *Upk1b*$^{RFP/RFP}$ bladder urothelium (**Figure 3**). Krt5 protein was increased in *Upk1b*$^{RFP/RFP}$ bladders, despite unchanged transcript levels (**Figure 3A-C**), and marked basolateral borders throughout multiple urothelial layers (**Figure 3I**). Krt14 mRNA, protein (**Figure 3A-C**) and total Krt14 basal cells (31.67 ± 7.055 *vs.* 4.667 ± 0.3333, p= 0.0187) were significantly increased compared to control (**Figure 3J, K**).

Upk1b$^{RFP/RFP}$ bladder urothelium exhibited a 5-fold increase in proliferation (**Figure 4A**, $p < 0.0001$), commonly associated with basal cells, but also some intermediate cells (**Supplemental Figure 3**). Expression of p63, a stem/progenitor marker,[18, 19] was expanded in *Upk1b*$^{RFP/RFP}$ basal and intermediate cell layers (**Figure 4C**). Re-expression of sonic hedgehog (Shh), a downstream transcriptional target of p63, was also observed where it uniformly marked basal and intermediate cells and localized to the basolateral surface of some superficial cells (**Figure 4E, F**).[20]

Kidney—*Upk1b*$^{RFP/+}$ and *Upk1b*$^{RFP/RFP}$ kidneys exhibited a graded decrease in *Upk1b* mRNA in conjunction with a graded increase in RFP expression (**Supplemental Figure 4**). RFP expression in *Upk1b*$^{RFP/+}$ and *Upk1b*$^{RFP/RFP}$ bladder lysates was 50- and 19-fold higher respectively, than the corresponding kidney samples, indicating urothelium comprises a smaller percentage of total kidney tissue than bladder and providing a rationale for the difficulty in detecting Upk proteins in kidneys.

Altered morphology and absent plaque

Upk1b$^{RFP/RFP}$ kidneys exhibit altered urothelial morphology with no defects observed in any other renal structures (**Supplemental Figure 4C-F**). *Upk1b*$^{RFP/RFP}$ urothelium appeared thickened, multilayered and contained apoptotic cells.

Upk1b$^{RFP/RFP}$ renal urothelium lacked surface plaques and the numerous fusiform vesicles and parallel membrane arrays observed in controls (**Figure 5A-B**), consistent with altered Upk expression (**Figure 5C-l**). *Upk3a*, *Upk3b*, *Upk1a* and *Upk2* mRNAs were significantly increased in *Upk1b*$^{RFP/RFP}$ kidneys (**Figure 5C**), although Upk3a protein was significantly decreased, as was Upk3a staining in *Upk1b*$^{RFP/RFP}$ renal urothelium (**Figure 5D, I**). Upk3b, Upk1a and Upk2 showed diffuse cytoplasmic expression in *Upk1b*$^{RFP/RFP}$ renal urothelium (**Figure 5F-L**), while Upk1a and Upk2 aberrantly localized to basolateral nuclear aggregates consistent with Golgi/ER entrapment (**Figure 5K, L**).[21]

Altered cellular composition

Urothelial organization was significantly altered in *Upk1b*$^{RFP/RFP}$ kidneys (**Figure 6**). *Krt20*, *Krt5* and *Krt14* mRNAs were significantly increased in *Upk1b*$^{RFP/RFP}$ kidneys (**Figure 6A**). Krt14 showed an increase in expression in *Upk1b*$^{RFP/RFP}$ kidneys (**Figure 6B**). Krt5 marked cortical basal cells beneath several layers of Krt5 negative cells, while increased Krt14 expression was detected in basal cells throughout *Upk1b*$^{RFP/RFP}$ renal urothelium (**Figure 6C-J**).

Hydronephrosis and CAKUT

Upk1b$^{RFP/RFP}$ mice developed progressive bilateral hydronephrosis with parenchymal thinning (**Figure 7, Tables 3 & 4**). Detrusor leak point pressure, bladder wall thickness, and voiding frequency and volume were unchanged in *Upk1b*$^{RFP/RFP}$ mice confirming a lack of lower urinary tract obstruction (unpublished data).

Approximately 16% of *Upk1b*$^{RFP/RFP}$ mice (14/85) had unilateral collecting system duplication (Fisher's exact test, $P < 0.0001$, **Figure 8**). Anterograde dye injection into the ectopic and orthotopic kidney pelvises revealed two patent ureters (**Figure 8D, E**). Retrograde dye injection from the bladder failed to identify the ectopic ureter, suggesting it did not insert into the bladder (unpublished data). Histology confirmed distinct renal pelvises separated by parenchymal septum (**Figure 8F**).

DISCUSSION

This study is the first to examine the functional consequences of genetic ablation of *Upk1b*, a unique tetraspanin Upk that can escape the ER without herterodimerization.[22] Loss of *Upk1b* expression in *Upk1b*$^{RFP/RFP}$ mice disrupted urothelial plaques throughout the urinary tract, consistent with its role in forming one of the key heterodimeric partners necessary for AUM formation. *Upk1b* is highly expressed in developing and mature urinary and reproductive tracts with significantly lower levels expression observed in other epithelial membranes and secretory organs. Although we focused on the urinary tract, survey of *Upk1b*$^{RFP/RFP}$ mice did not detect deficits associated with any other organs/tissues.

The primary defects observed in *Upk1b*$^{RFP/RFP}$ mice appear cell-autonomous and were directly associated with loss of *Upk1b* expression and plaque formation resulting in urothelial dysmorphogenesis, loss of urothelial structural integrity and a novel association of Upk1b with the development of CAKUT. These observations are consistent with the proposed mechanistic actions of Upks: 1) regulation of membrane permeability, 2) stabilization of the apical membrane through AUM/cytoskeletal interactions, and 3) mediation of signaling events regulating cellular development, activity, growth and motility.[2, 3]

The primary mechanistic action of Upk1b in urothelium resides in its role in forming plaques.[2] Prior studies have shown that disruption of the AUM results in alterations in urothelial morphology.[4, 5] A similar mechanism is proposed for *Upk1b*$^{RFP/RFP}$ mice, where absence of urothelial plaques prevents development of the permeability barrier. As a result, umbrella cells are exposed to urine causing cellular damage and loss. These defects result in alterations in cellular phenotype within the urothelium of both kidney and bladder (Figure 9). Urothelium in *Upk1b*$^{RFP/RFP}$ mice is less mature resulting a multilayered renal urothelium that appears bladder-like and a highly disorganized bladder urothelium that is dysplastic.

The precise signals causing the morphologic changes observed in *Upk1b*$^{RFP/RFP}$ urothelium are likely multifactorial, involving intrinsic and extrinsic factors. Studies indicate Upk proteins have intrinsic signaling capabilities; Upk3a possesses a cytoplasmic signaling domain that is important in mediating bacterial invasion and apoptosis.[23] Bacterial binding to Upk1a induces transcriptional changes in basal and intermediate cells before umbrella cells were compromised.[2] Therefore, lack of plaques in *Upk1b*$^{RFP/RFP}$ mice would prevent these intrinsic signaling pathways. It seems reasonable to assume that at least some of these intrinsic signals are critical for the development and maintenance of the superficial cell phenotype, thereby providing a mechanism for their loss in *Upk1b*$^{RFP/RFP}$ mice. This fact is likely compounded by cellular damage and loss associated with urine exposure resulting in exacerbation of the phenotype based upon the secondary extrinsic signaling pathways associated with normal urothelial development, stratification and homeostasis.

One clear product of *Upk1b* ablation in *Upk1b*$^{RFP/RFP}$ mice is increased proliferation and cellularity within the urothelium of both the kidney and bladder. The primary cell types associated with this increase in proliferation were the Krt5 and Krt14 basal cells, which is consistent with the tissue-specific expansion of these progenitors following a variety of injury models.[7, 8, 24, 25] These observations are also supported by studies in our lab where urothelial remodeling in hydronephrotic kidneys involved increased urothelial proliferation in Krt14-expressing cells, urothelial stratification, and *de novo* Upk expression.[6]

We hypothesize that urothelial plaques represent the functional equivalent of an apical basement membrane that is necessary for normal development and maintenance of superficial cells lining the urinary tract. Plaque destabilization has the potential to alter signaling pathways associated with normal urothelial development and homeostasis. Depending upon the insult, these alterations in signaling may involve both intrinsic and extrinsic pathways and thereby elicit distinct injury responses. For example, *Upk1b* ablation

and bacterial binding may interrupt a negative feedback loop that keeps Krt5-expressing basal cells quiescent resulting in their rapid expansion.[24] By comparison, intermediate cells already express Upks and rapidly replace superficial cells following chemical injury, thereby preserving the negative feedback loop and keeping Krt5 progenitors quiescent.[25]

This model is supported by the observation that *Upk1b*$^{RFP/RFP}$ mice possess dysplastic urothelium, a feature postulated as a precursor of carcinoma *in-situ* and invasive bladder cancer.[26, 27] Prior studies suggested Upks, including Upk1b,[28] are tumor suppressor genes, and individual cell types have been implicated in chemically-induced bladder cancers.[29, 30] Our data supports this and provides novel evidence that absent *Upk1b* expression results in urothelial dysplasia.

The fact that *Upk1b*$^{RFP/RFP}$ mice develop spontaneous, age-dependent, progressive hydronephrosis in the absence of obstruction indicates the defect is a direct, cell-autonomous consequence of *Upk1b* loss. Association of the AUM's with intracellular cytoskeletal elements is thought to stabilize apical membranes and increase structural integrity of the urothelium during pressure fluctuations associated with urine storage and micturition. We hypothesize that *Upk1b*$^{RFP/RFP}$ mice possess weakened urothelial integrity due to plaque loss that leads to a structurally and functionally deficient urothelium. As postnatal nephrogenesis progresses and glomerular filtration rate increases, increased urine production and storage pressure gradually stresses *Upk1b*$^{RFP/RFP}$ urothelium resulting in the onset of spontaneous progressive hydronephrosis observed in these animals. The kidney may be particularly sensitive since it lacks the well-defined muscular coat.

The unexpected observation that *Upk1b* ablation results in duplex kidneys indicates that Upk1b expression is necessary for normal ureteric bud formation. Nothing is currently known regarding Upk expression during early urinary tract development, but a variety of supportive evidence suggests they play a role. Upk3a is expressed in the urinary tract of *Xenopus*, and *upk3l* (*Upk3a-like*) morpholinos affect zebrafish pronephros development.[31, 32] In addition, heterozygous *UPK3A* mutations associate with renal adyspasia and/or vericoureteral reflux,[33] while *UPK2* mutations associate with renal malformations in humans[34] and common genetic variants in *UPK3A* trended toward an association with duplex kidneys in a Dutch population.[35] These studies and our results support an expanded role for Upks in urinary tract development and CAKUT.

This study indicates that *Upk1b* expression is critical for urothelial plaque stability, maturation, differentiation and homeostasis of urothelium. We demonstrate that urothelium is regionally distinct and highly plastic, possessing the potential to modify its cellular composition based upon expansion of specific cell populations. We provide the first experimental evidence that Upks function in kidney development and in the formation of CAKUT. These observations mechanistically link developmental defects of the urinary tract (duplex kidney), functional deficits within the urinary tract (spontaneous hydronephrosis) and urothelial dysplasia. Linking these disparate clinical entities to a single genetic loci provides a unique pathogenic paradigm for urinary tract diseases and may be critical in directed follow-up treatment of patients. Future studies will define the functional role that *Upk1b* plays in urinary tract development and reexamine potential genetic and epigenetic

association of Upks with a variety of urinary tract diseases/disorders in hopes of identifying common pathogenic processes.

MATERIALS AND METHODS

Ethics Statement

Animal studies were conducted under Public Health Services Animal Welfare Assurance number A3544-01, and approved by Institutional Animal Care and Use Committee protocol 02105AR.

Animals

Upk1b^{tm1Pzg}/J mice generated by the GenitoUrinary Development Molecular Anatomy Project (GUDMAP) consortium[36] (hereafter called *Upk1b*$^{+/+}$, *Upk1b*$^{RFP/+}$, *Upk1b*$^{RFP/RFP}$) were backcrossed to an FVB/N. Red fluorescent protein and polyadenylation sequence (RFP-pA) disrupts Upk1b translation. RFP-carrying mutants express RFP from the endogenous *Upk1b* promoter. GUDMAP validated that the RFP knock-in localizes to expected tissues and the allele exhibits expected activity (www.gudmap.org/Docs/Mouse_Strains/Upk1b_RFP_Report.pdf), and we confirmed this in FVB/N backcrossed mice. *Upk1b*$^{+/+}$, *Upk1b*$^{RFP/+}$ and *Upk1b*$^{RFP/RFP}$ were examined; data is reported for *Upk1b*$^{RFP/+}$ when it's significantly altered versus control. Data presented represents 2-3 months old mice; however urothelial changes were observed at postnatal day (P)7-P10, prior to onset of hydronephrosis (**Supplemental Figure 5**). This study is limited to bladder and kidney; however, we observed no other organ defects through gross evaluation.

Histology & Immunohistochemistry

RFP was observed by mounting deparaffinized and rehydrated tissue sections with VECTASHIELD® with DAPI (Vector Laboratories, Burlingame, CA), and imaged using a Spot Camera and Leica DM4000B microscope. Routine H&E was performed and evaluated by a certified veterinary pathologist (CPMPSR, Ohio State University, Columbus, OH, **Table 1**).

Immunohistochemistry was performed as previously described.[6, 37, 38] Primary antibodies: Upk1a, Upk2, Upk3b, Shh, p63 (Santa Cruz Biotechnology, Santa Cruz, CA), Upk3a (Fitzgerald Industries International, Acton, MA), Krt13, Krt5, Krt14 (Covance, Princeton, NJ), and Krt20 (Dako North America, Inc., Carpinteria, CA) were detected using Anti-Polyvalent or Anti-Goat and, HRP/DAB reagents (Scytek Laboratories, Logan, UT). Sections were imaged using an Olympus BX51 microscope and CX9000 camera. Krt14 positive cells were quantitated in random high power fields (40×). Statistical significance was determined using an unpaired two-tailed *t* test.

Proliferation was detected using the Click-iT® EdU Alexa Fluor® 488 Imaging Kit per manufacturers recommendation (Life Technologies, Carlsbad, CA). 500μg 5-ethynyl-2′-deoxyuridine (EdU) was administered via intraperitoneal injection. Mice were euthanized after two hours, tissues were sectioned and EdU detection was performed at 250μm

intervals. Percentage of EdU-positive urothelial cells was quantitated. A two-way ANOVA was used to calculate p-values (Version 6.0c, GraphPad Software, Inc., La Jolla, CA).

Immunoblotting

Total protein was procured, denatured, resolved by SDS-PAGE and transferred to PVDF membrane (Bio-Rad Laboratories, Inc., Hercules, CA). Primary antibody: Upk1a, Upk2, Upk3a, Upk3b, Krt5, Krt14, Krt20, Shh, RFP (Rockland Immunochemicals, Inc. Gilbertsville, PA), and GAPDH (EMD Millipore, Billerica, MA) was incubated overnight, followed by two hour incubation with HRP-conjugated secondaries (Vector Laboratories). Proteins were visualized using ECL and chemiluminescence film.

Ultrasonography

Hydronephrosis was measured using the Vevo 2100 as previously described.[39] Average percent parenchyma ± SEM was graphed, and a two-way ANOVA was performed. Bladder wall thickness was measured during ultrasonography. Average thickness ± SD was graphed, and a t-test was performed.

Transmission Electron Microscopy

Tissues were perfused with PBS and 2% glutaraldehyde/PBS, fixed in 2.5% glutaraldehyde, post-fixed in 1% osmium tetroxide, dehydrated in ethanols, cleared in propylene oxide and infiltrated with 1:1 Epon/Araldite:propylene oxide and Epon/Araldite. 60nm sections were collected onto CuPd grids, stained with uranyl acetate and lead citrate, viewed on a Hitachi H 7650 (Hitachi, Ltd.,Chiyoda, Tokyo), and evaluated by a certified veterinary pathologist.

Quantitative PCR (qPCR)

qPCR was performed as previously described.[6] 12.5ng of cDNA and gene-specific primers/probes were used (Roche NimbleGen, Incorporated, Madison, WI). Triplicate reactions included *Gapdh*. Results were expressed using the 2^{-CT} method by normalizing to control kidney or bladder cDNA. Average fold change ± SEM and a two-way ANOVA was performed.

Supplementary Material

Refer to Web version on PubMed Central for supplementary material.

ACKNOWLEDGEMENTS

We would like to thank Jim Lessard, PhD for providing the FVB/N backcrossed mice for this study. We would like to thank Brad Bolon DVM, MS, PhD at The Ohio State University Comparative Pathology & Mouse Phenotyping Shared Resource for careful evaluation of the H&E and TEM preparations. We would also like to thank Cindy McAllister in the Morphology Core at The Research Institute at Nationwide Children's Hospital for help in preparing samples for TEM. Finally, funding for this work was supported by NIH R01-DK70907 and R01-DK085242.

REFERENCES

1. Batourina E, Tsai S, Lambert S, et al. Apoptosis induced by vitamin A signaling is crucial for connecting the ureters to the bladder. Nature genetics. 2005; 37:1082–1089. [PubMed: 16186816]

2. Khandelwal P, Abraham SN, Apodaca G. Cell biology and physiology of the uroepithelium. American journal of physiology Renal physiology. 2009; 297:F1477–1501. [PubMed: 19587142]
3. Wu XR, Kong XP, Pellicer A, et al. Uroplakins in urothelial biology, function, and disease. Kidney international. 2009; 75:1153–1165. [PubMed: 19340092]
4. Hu P, Deng FM, Liang FX, et al. Ablation of uroplakin III gene results in small urothelial plaques, urothelial leakage, and vesicoureteral reflux. The Journal of cell biology. 2000; 151:961–972. [PubMed: 11085999]
5. Kong XT, Deng FM, Hu P, et al. Roles of uroplakins in plaque formation, umbrella cell enlargement, and urinary tract diseases. The Journal of cell biology. 2004; 167:1195–1204. [PubMed: 15611339]
6. Becknell B, Carpenter AR, Allen JL, et al. Molecular basis of renal adaptation in a murine model of congenital obstructive nephropathy. PloS one. 2013; 8:e72762. [PubMed: 24023768]
7. Girshovich A, Vinsonneau C, Perez J, et al. Ureteral obstruction promotes proliferation and differentiation of the renal urothelium into a bladder-like phenotype. Kidney international. 2012; 82:428–435. [PubMed: 22513823]
8. Vinsonneau C, Girshovich A, M'Rad M B, et al. Intrarenal urothelium proliferation: an unexpected early event following ischemic injury. American journal of physiology Renal physiology. 2010; 299:F479–486. [PubMed: 20591940]
9. Wu XR, Lin JH, Walz T, et al. Mammalian uroplakins. A group of highly conserved urothelial differentiation-related membrane proteins. The Journal of biological chemistry. 1994; 269:13716–13724. [PubMed: 8175808]
10. Deng FM, Liang FX, Tu L, et al. Uroplakin IIIb, a urothelial differentiation marker, dimerizes with uroplakin Ib as an early step of urothelial plaque assembly. The Journal of cell biology. 2002; 159:685–694. [PubMed: 12446744]
11. Wu XR, Manabe M, Yu J, et al. Large scale purification and immunolocalization of bovine uroplakins I, II, and III. Molecular markers of urothelial differentiation. The Journal of biological chemistry. 1990; 265:19170–19179. [PubMed: 2229070]
12. Yu J, Lin JH, Wu XR, et al. Uroplakins Ia and Ib, two major differentiation products of bladder epithelium, belong to a family of four transmembrane domain (4TM) proteins. The Journal of cell biology. 1994; 125:171–182. [PubMed: 8138569]
13. Yu J, Manabe M, Wu XR, et al. Uroplakin I: a 27-kD protein associated with the asymmetric unit membrane of mammalian urothelium. The Journal of cell biology. 1990; 111:1207–1216. [PubMed: 1697295]
14. Hu CC, Liang FX, Zhou G, et al. Assembly of urothelial plaques: tetraspanin function in membrane protein trafficking. Molecular biology of the cell. 2005; 16:3937–3950. [PubMed: 15958488]
15. Tu L, Sun TT, Kreibich G. Specific heterodimer formation is a prerequisite for uroplakins to exit from the endoplasmic reticulum. Molecular biology of the cell. 2002; 13:4221–4230. [PubMed: 12475947]
16. Wu XR, Medina JJ, Sun TT. Selective interactions of UPIa and UPIb, two members of the transmembrane 4 superfamily, with distinct single transmembrane-domained proteins in differentiated urothelial cells. The Journal of biological chemistry. 1995; 270:29752–29759. [PubMed: 8530366]
17. Garcia-Espana A, Chung PJ, Zhao X, et al. Origin of the tetraspanin uroplakins and their co-evolution with associated proteins: implications for uroplakin structure and function. Molecular phylogenetics and evolution. 2006; 41:355–367. [PubMed: 16814572]
18. Karni-Schmidt O, Castillo-Martin M, Shen TH, et al. Distinct expression profiles of p63 variants during urothelial development and bladder cancer progression. The American journal of pathology. 2011; 178:1350–1360. [PubMed: 21356385]
19. Pignon JC, Grisanzio C, Geng Y, et al. p63-expressing cells are the stem cells of developing prostate, bladder, and colorectal epithelia. Proceedings of the National Academy of Sciences of the United States of America. 2013; 110:8105–8110. [PubMed: 23620512]
20. Caserta TM, Kommagani R, Yuan Z, et al. p63 overexpression induces the expression of Sonic Hedgehog. Molecular cancer research : MCR. 2006; 4:759–768. [PubMed: 17050669]

21. Hudoklin S, Zupancic D, Romih R. Maturation of the Golgi apparatus in urothelial cells. Cell and tissue research. 2009; 336:453–463. [PubMed: 19370362]
22. Tu L, Kong XP, Sun TT, et al. Integrity of all four transmembrane domains of the tetraspanin uroplakin Ib is required for its exit from the ER. Journal of cell science. 2006; 119:5077–5086. [PubMed: 17158912]
23. Thumbikat P, Berry RE, Zhou G, et al. Bacteria-induced uroplakin signaling mediates bladder response to infection. PLoS pathogens. 2009; 5:e1000415. [PubMed: 19412341]
24. Shin K, Lee J, Guo N, et al. Hedgehog/Wnt feedback supports regenerative proliferation of epithelial stem cells in bladder. Nature. 2011; 472:110–114. [PubMed: 21389986]
25. Gandhi D, Molotkov A, Batourina E, et al. Retinoid signaling in progenitors controls specification and regeneration of the urothelium. Developmental cell. 2013; 26:469–482. [PubMed: 23993789]
26. Cheng L, Cheville JC, Neumann RM, et al. Natural history of urothelial dysplasia of the bladder. The American journal of surgical pathology. 1999; 23:443–447. [PubMed: 10199474]
27. Siegel R, Naishadham D, Jemal A. Cancer statistics, 2013. CA: a cancer journal for clinicians. 2013; 63:11–30. [PubMed: 23335087]
28. Finch JL, Miller J, Aspinall JO, et al. Cloning of the human uroplakin 1B cDNA and analysis of its expression in urothelial-tumor cell lines and bladder-carcinoma tissue. International journal of cancer Journal international du cancer. 1999; 80:533–538. [PubMed: 9935153]
29. Becci PJ, Thompson HJ, Strum JM, et al. N-butyl-N-(4-hydroxybutyl)nitrosamine-induced urinary bladder cancer in C57BL/6 X DBA/2 F1 mice as a useful model for study of chemoprevention of cancer with retinoids. Cancer research. 1981; 41:927–932. [PubMed: 7459879]
30. Van Batavia J, Yamany T, Molotkov A, et al. Bladder cancers arise from distinct urothelial sub-populations. Nature cell biology. 2014; 16:982–991. [PubMed: 25218638]
31. Mitra S, Lukianov S, Ruiz WG, et al. Requirement for a uroplakin 3a-like protein in the development of zebrafish pronephric tubule epithelial cell function, morphogenesis, and polarity. PloS one. 2012; 7:e41816. [PubMed: 22848617]
32. Sakakibara K, Sato K, Yoshino K, et al. Molecular identification and characterization of Xenopus egg uroplakin III, an egg raft-associated transmembrane protein that is tyrosine phosphorylated upon fertilization. The Journal of biological chemistry. 2005; 280:15029–15037. [PubMed: 15699050]
33. Jenkins D, Bitner-Glindzicz M, Malcolm S, et al. De novo Uroplakin IIIa heterozygous mutations cause human renal adysplasia leading to severe kidney failure. Journal of the American Society of Nephrology : JASN. 2005; 16:2141–2149. [PubMed: 15888565]
34. Jenkins D, Bitner-Glindzicz M, Malcolm S, et al. Mutation analyses of Uroplakin II in children with renal tract malformations. Nephrology, dialysis, transplantation : official publication of the European Dialysis and Transplant Association - European Renal Association. 2006; 21:3415–3421.
35. van Eerde AM, Duran K, van Riel E, et al. Genes in the ureteric budding pathway: association study on vesico-ureteral reflux patients. PloS one. 2012; 7:e31327. [PubMed: 22558067]
36. McMahon AP, Aronow BJ, Davidson DR, et al. GUDMAP: the genitourinary developmental molecular anatomy project. Journal of the American Society of Nephrology : JASN. 2008; 19:667–671. [PubMed: 18287559]
37. Carpenter A, Paulus A, Robinson M, et al. 3-Dimensional morphometric analysis of murine bladder development and dysmorphogenesis. Developmental dynamics : an official publication of the American Association of Anatomists. 2012; 241:522–533. [PubMed: 22275180]
38. Ingraham SE, Saha M, Carpenter AR, et al. Pathogenesis of renal injury in the megabladder mouse: a genetic model of congenital obstructive nephropathy. Pediatric research. 2010; 68:500–507. [PubMed: 20736884]
39. Carpenter AR, Becknell B, Ingraham SE, et al. Ultrasound imaging of the murine kidney. Methods in molecular biology. 2012; 886:403–410. [PubMed: 22639280]

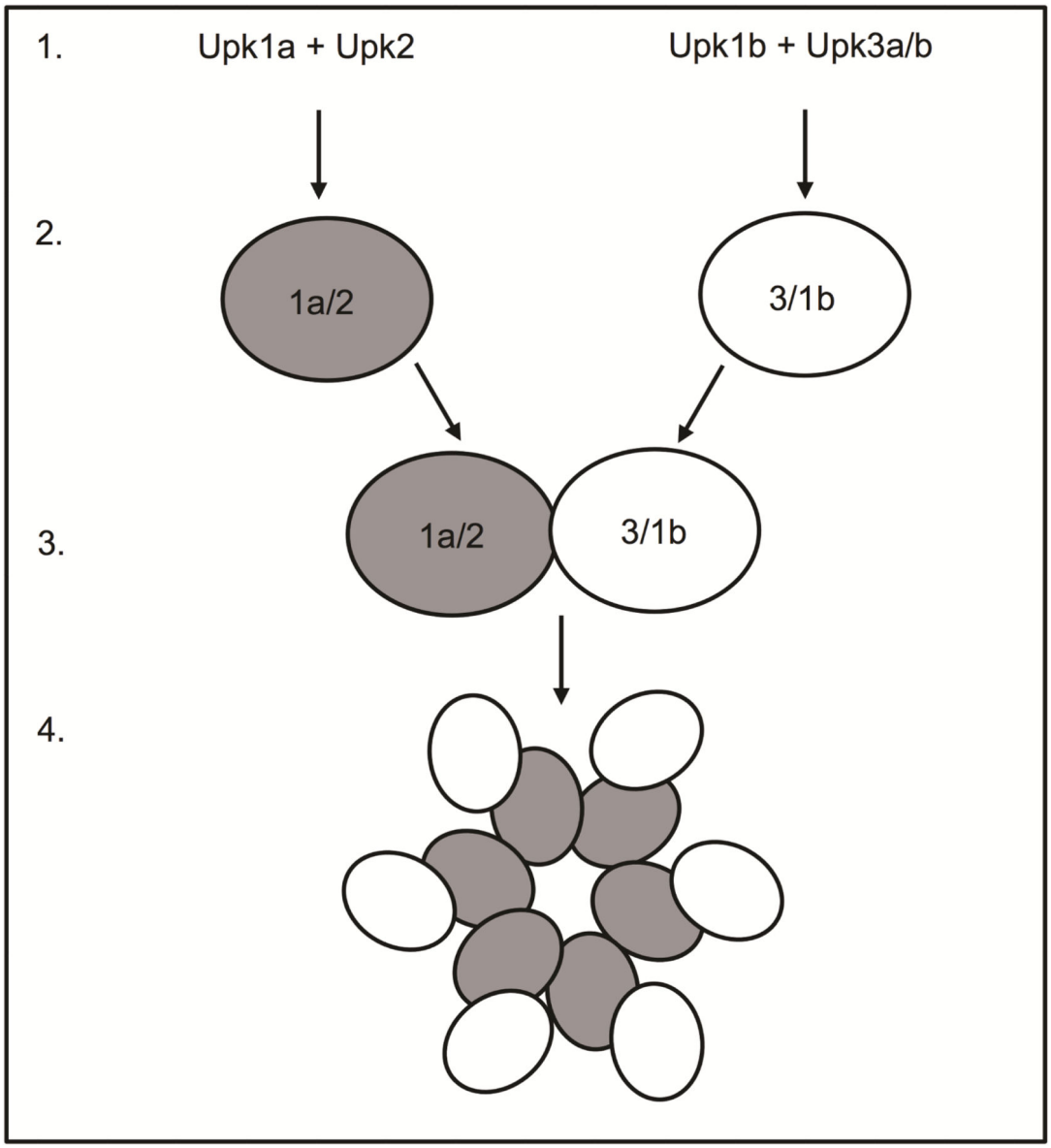

Figure 1. Urothelial plaque assembly

Schematic depiction of urothelial plaque assembly from (1) uroplakin assembly in the endoplasmic reticulum, to (2) heterodimerization, (3) heterotetramerization and (4) particle formation.

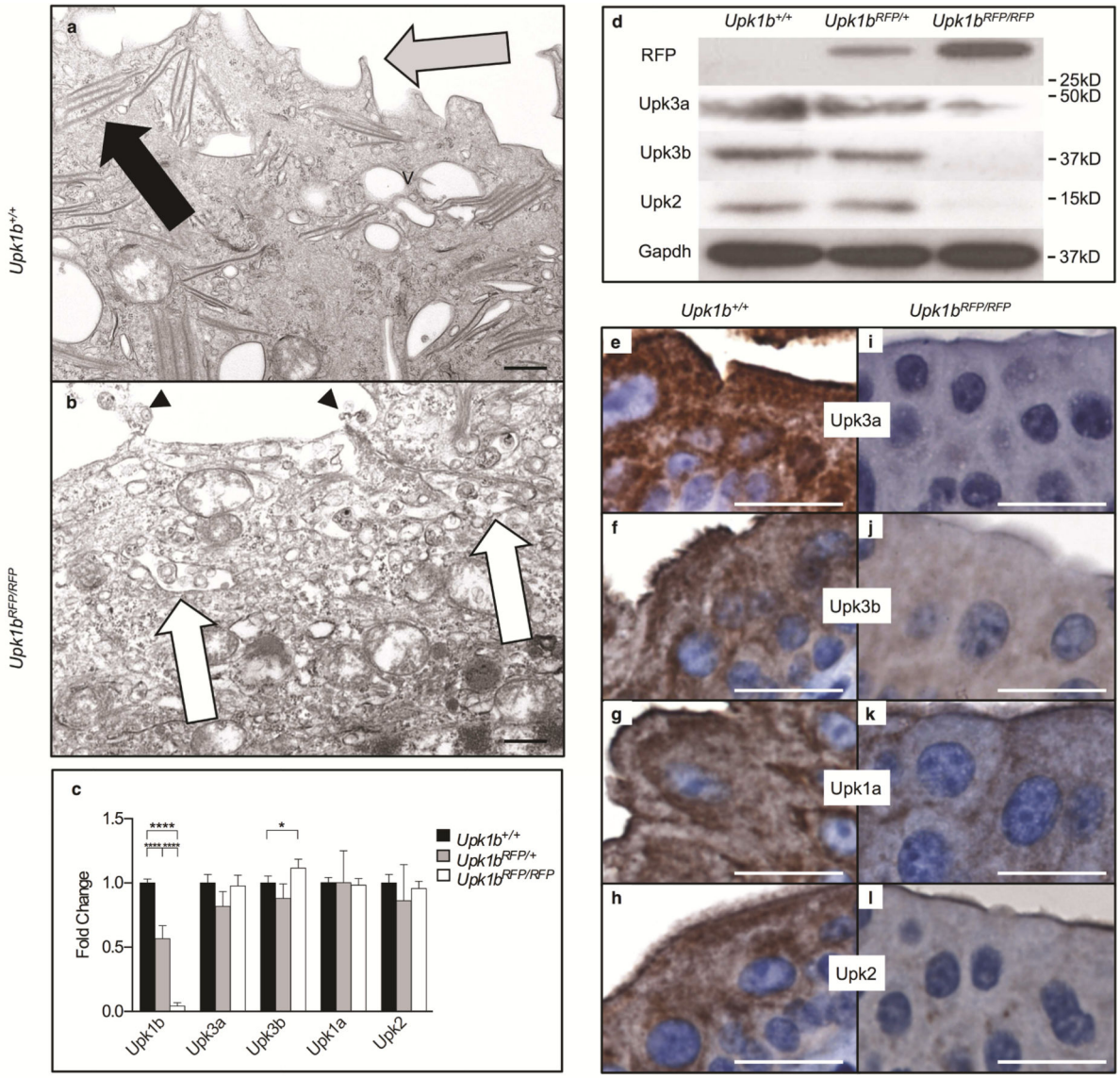

Figure 2. RFP-disrupted *Upk1b* Leads to Defective Urothelial Plaque

(A, B) Ultrastructural analysis of the apical surface of the urothelial superficial cell layer in *Upk1b*$^{+/+}$ and *Upk1b*$^{RFP/RFP}$ bladders was assessed by transmission electron microscopy. V: discoid and fusiform vesicles, Black Arrow: Parallel membranes, Gray Arrow: Pointed Apical Projections, Arrowhead: Blunted Apical Projections, White Arrow: Membranous Body Containing Vesicles. (C) Uroplakin expression in *Upk1b*$^{+/+}$, *Upk1b*$^{RFP/+}$ and *Upk1b*$^{RFP/RFP}$ bladders (*n*=3 *Upk1b*, *n*=5 *Upk3a*, *Upk3b*, *Upk1a*, *Upk2*) was measured by qPCR. Raw data was normalized to *Gapdh* and fold change relative to *Upk1b*$^{+/+}$ is graphed. A Two-Way ANOVA and Tukey's multiple comparison post-hoc test were used to evaluate statistical significance. *$p < 0.05$, ****$p < 0.0001$. Error bars represent standard error. (D) Protein expression in *Upk1b*$^{+/+}$, *Upk1b*$^{RFP/+}$ and *Upk1b*$^{RFP/RFP}$ bladders were analyzed by immunoblotting using the antibodies indicated. (E-L) Superficial and intermediate cell morphology in *Upk1b*$^{+/+}$ and *Upk1b*$^{RFP/RFP}$ bladders were analyzed by

immunohistochemistry for the antibodies indicated. Scale bars indicate 500nm (A, B), 25μm (E-L).

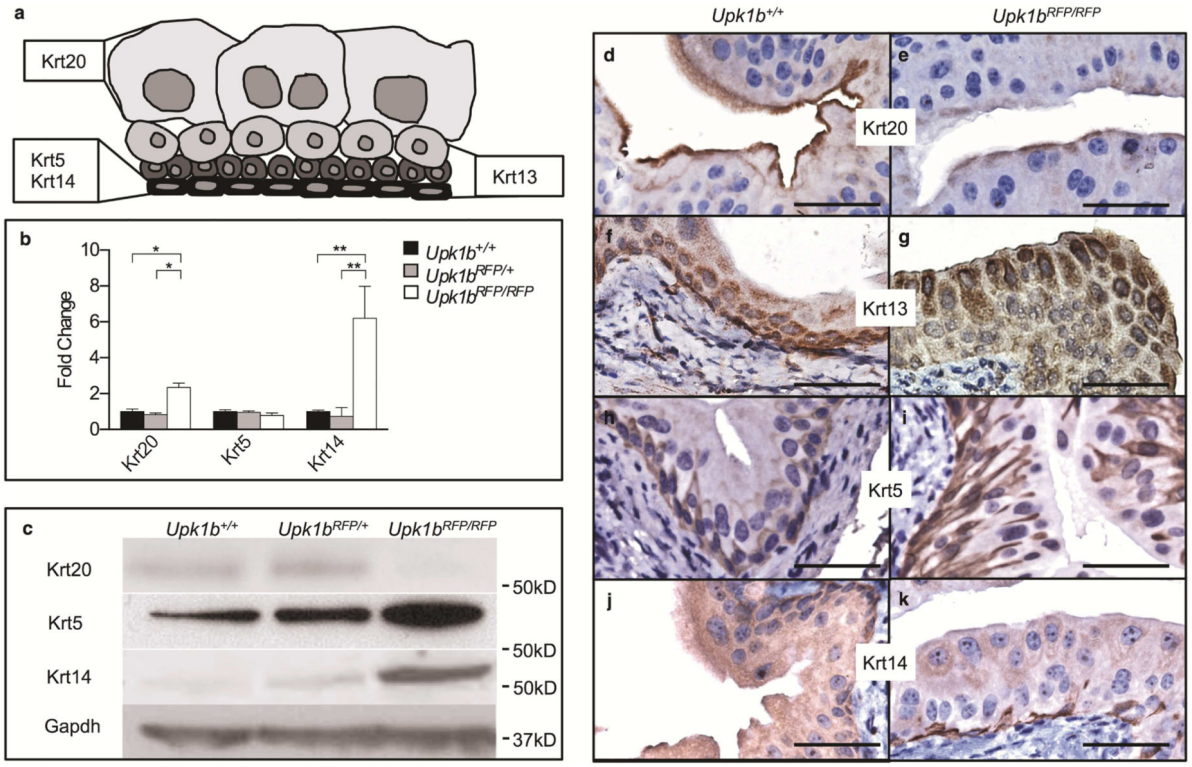

Figure 3. Absent *Upk1b* and Urothelial Plaque Affect Urothelial Homeostasis, Maturation and Organization

(A) Schematic of urothelial cell morphology including the previously reported cytokeratin (Krt) profiles of basal, intermediate and umbrella cells. The cytokeratins used for immunohistochemistry are indicated in bold. (B) Cytokeratin mRNA expression in $Upk1b^{+/+}$, $Upk1b^{RFP/RFP}$ and $Upk1b^{+/+}$ bladders (n=5) was analyzed by qPCR. Raw data was normalized to *Gapdh* and fold change relative to $Upk1b^{+/+}$ is graphed. A Two-Way ANOVA and Tukey's multiple comparison post-hoc test were used to evaluate statistical significance. *$p < 0.05$, **$p < 0.01$. Error bars represent standard error. (C) Protein expression in $Upk1b^{+/+}$, $Upk1b^{RFP/+}$ and $Upk1b^{RFP/RFP}$ bladders was evaluated by immunoblotting for the antibodies indicated. (D-K) Urothelial morphology in $Upk1b^{+/+}$, $Upk1b^{RFP/RFP}$ bladders was analyzed by immunohistochemistry for the antibodies indicated. Scale bars indicate 25μm.

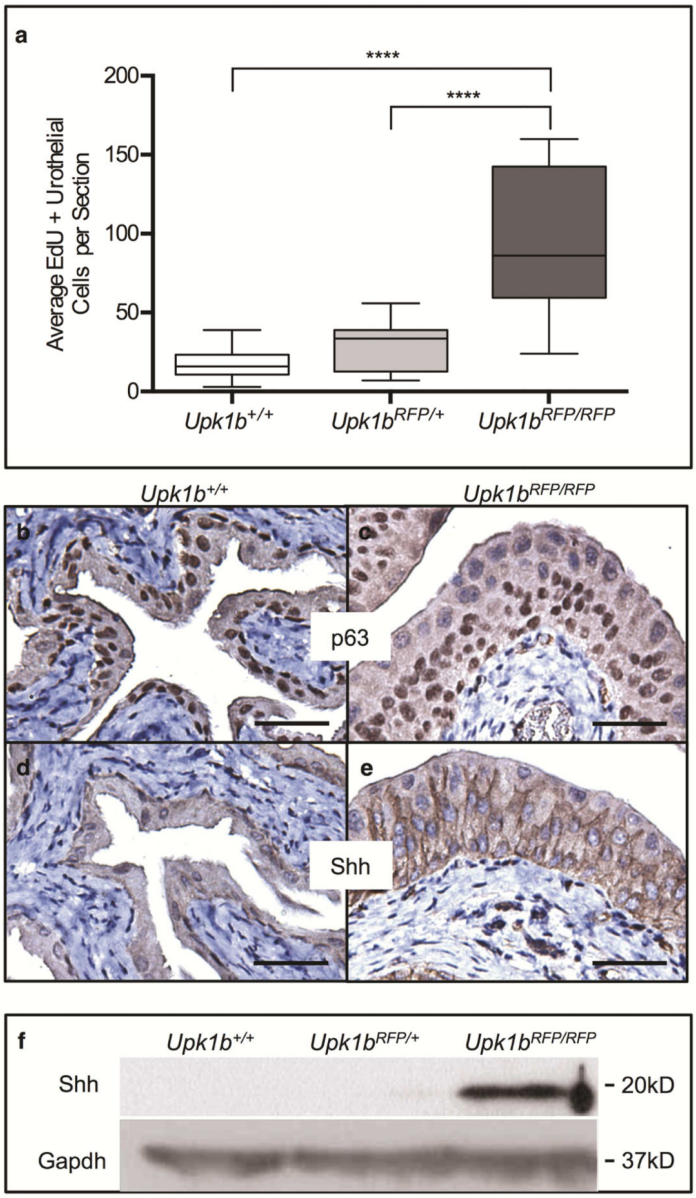

Figure 4. Absent *Upk1b* and Urothelial Plaque Increase Urothelial Proliferation

(A) A box and whiskers plot displays the average EdU+ urothelial cells (UCs) per section in $Upk1b^{+/+}$, $Upk1b^{RFP/+}$ and $Upk1b^{RFP/RFP}$ bladders (n=3). Whiskers represent the minimum and maximum. A two-way ANOVA in conjunction with Tukey's multiple comparison correction was used to calculate p-values. ****$p < 0.0001$. (B-E) Expression of p63 and the downstream target Shh were evaluated in $Upk1b^{+/+}$ and $Upk1b^{RFP/RFP}$ bladder urothelium by immunohistochemistry. (F) Protein expression in $Upk1b^{+/+}$, $Upk1b^{RFP/+}$ and $Upk1b^{RFP/RFP}$ bladders was evaluated by immunoblotting for Shh and Gapdh. Scale bars indicate 25μm (B-E).

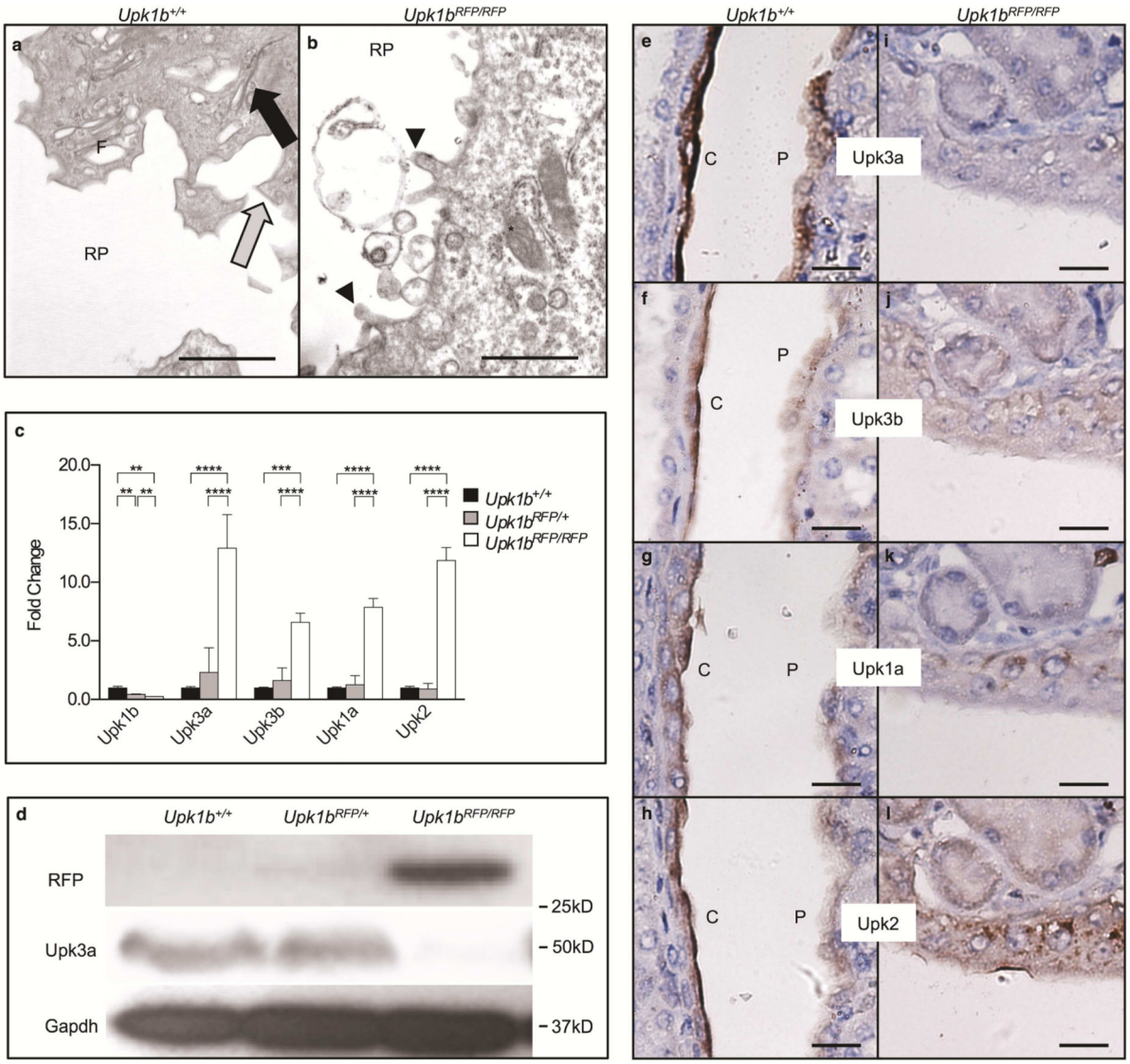

Figure 5. RFP-disrupted *Upk1b* Leads to Defective Urothelial Plaque in the Kidneys

(A, B) Ultrastructural analysis of the apical surface of the cortical, renal urothelial superficial cell layer in *Upk1b*$^{+/+}$ and *Upk1b*$^{RFP/RFP}$ kidneys was assessed by transmission electron microscopy. RP: Renal Pelvis, Black Arrow: Parallel membranes, Gray Arrow: Pointed Apical Projections, Arrowhead: Blunted Apical Projections, F: Fusiform Vesicles. Asterisk: Mitochondria. (C) Uroplakin mRNA expression in *Upk1b*$^{+/+}$, *Upk1b*$^{RFP/+}$ and *Upk1b*$^{RFP/RFP}$ kidneys was evaluated by qPCR (n=3 *Upk1b*, n=6 *Upk3a*, *Upk3b*, *Upk1a*, *Upk2*). Raw data was normalized to *Gapdh* and fold change relative to *Upk1b*$^{+/+}$ is graphed. A Two-Way ANOVA and Tukey's multiple comparison post-hoc test were used to evaluate statistical significance. *p < 0.05, **p < 0.01, ***p < 0.001., ****p < 0.0001. Error bars represent standard error. (D) Protein expression in *Upk1b*$^{+/+}$, *Upk1b*$^{RFP/+}$ and *Upk1b*$^{RFP/RFP}$ kidneys was evaluated by immunoblotting for the antibodies indicated. (E-L) Renal urothelial morphology in *Upk1b*$^{+/+}$ and *Upk1b*$^{RFP/RFP}$ kidneys was evaluated by

immunohistochemistry for the antibodies indicated. Scale bar indicates 1μm (A, B), 25μm (E-L).

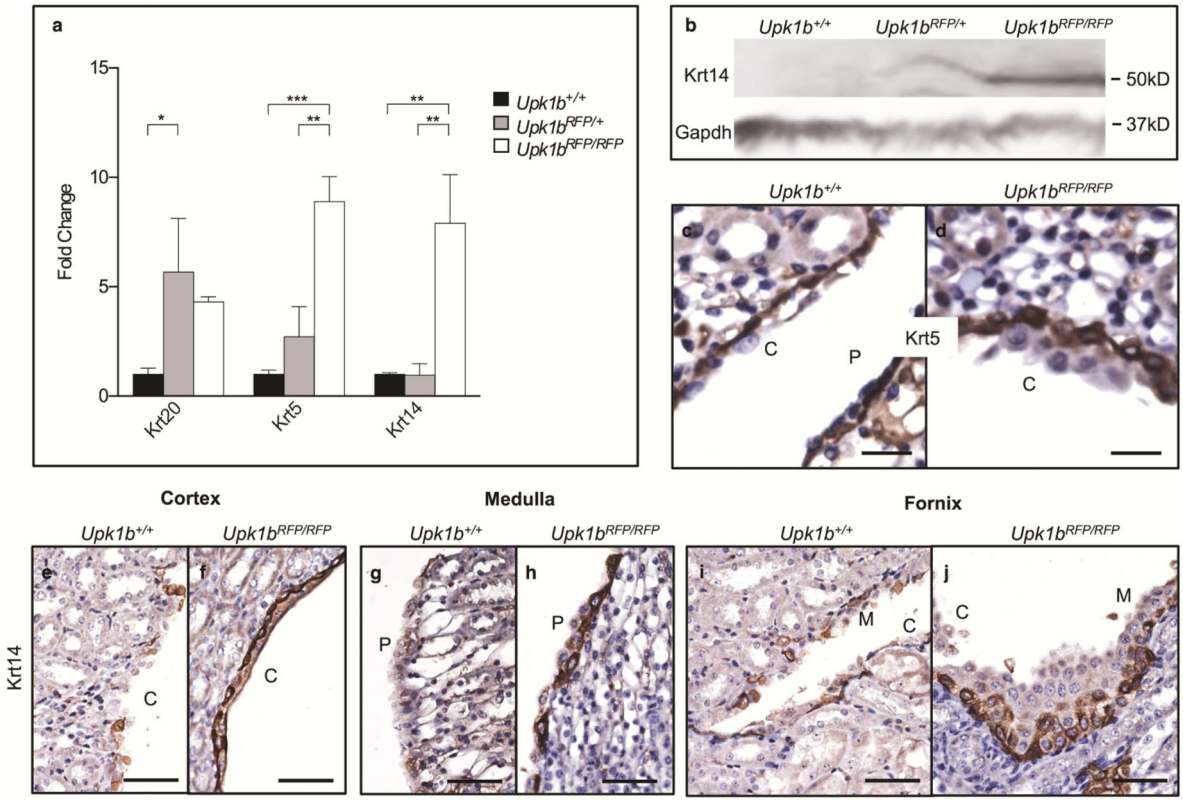

Figure 6. Absent *Upk1b* and Urothelial Plaque Affect Renal Urothelial Composition and Organization

(A) Cytokeratin mRNA expression in *Upk1b*$^{+/+}$, *Upk1b*$^{RFP/+}$ and *Upk1b*$^{RFP/RFP}$ kidneys (*n*=3) was analyzed by qPCR. Raw data was normalized to *Gapdh* and fold change relative to *Upk1b*$^{+/+}$ is graphed. A Two-Way ANOVA and Tukey's multiple comparison post-hoc test were used to evaluate statistical significance. *p < 0.05, **p < 0.01, ***p < 0.001. Error bars represent standard error. (B) Protein expression in *Upk1b*$^{+/+}$, *Upk1b*$^{RFP/+}$ and *Upk1b*$^{RFP/RFP}$ kidneys was evaluated by immunoblotting for Krt14 and Gapdh. (C-J) Krt5 and Krt14 expression in *Upk1b*$^{+/+}$ and *Upk1b*$^{RFP/RFP}$ renal urothelium was analyzed by immunohistochemistry. C: Cortical Urothelium, P: Papillary Urothelium. Scale bars indicate 25μm (C-D) 50μm (E-J).

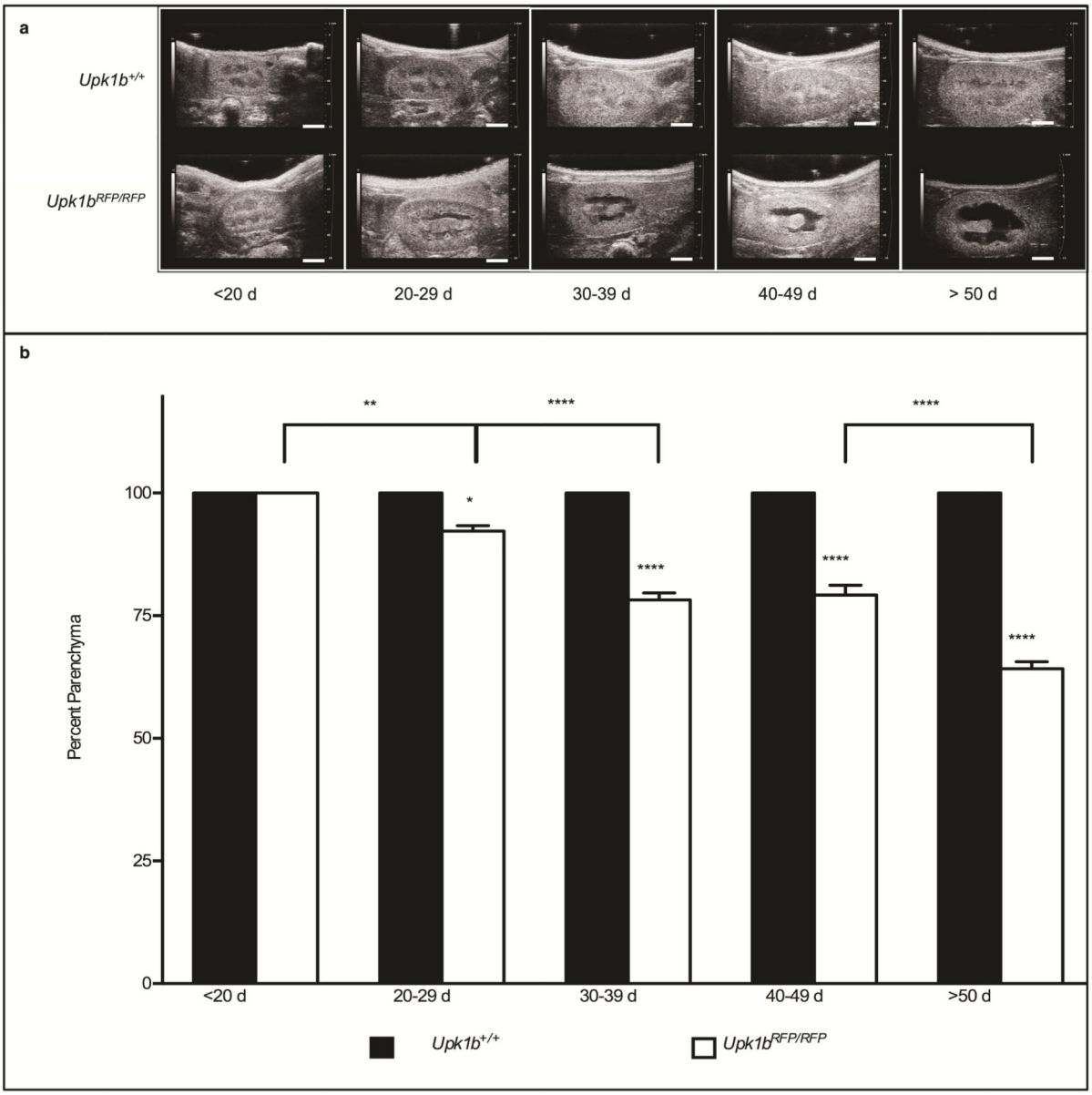

Figure 7. Absent *Upk1b* and Urothelial Plaque Affect Renal Structure

(A) Renal ultrasound was used to analyze hydronephrosis in *Upk1b*$^{+/+}$ and *Upk1b*$^{RFP/RFP}$ mice at the ages indicated. (B) Data is represented as the percent parenchyma (n>18). A Two-Way ANOVA and Tukey's multiple comparison post-hoc test were used to evaluate statistical significance. *p < 0.05 **p < 0.01 ****p < 0.0001. Error bars represent standard error. Scale bars indicate 2mm (A).

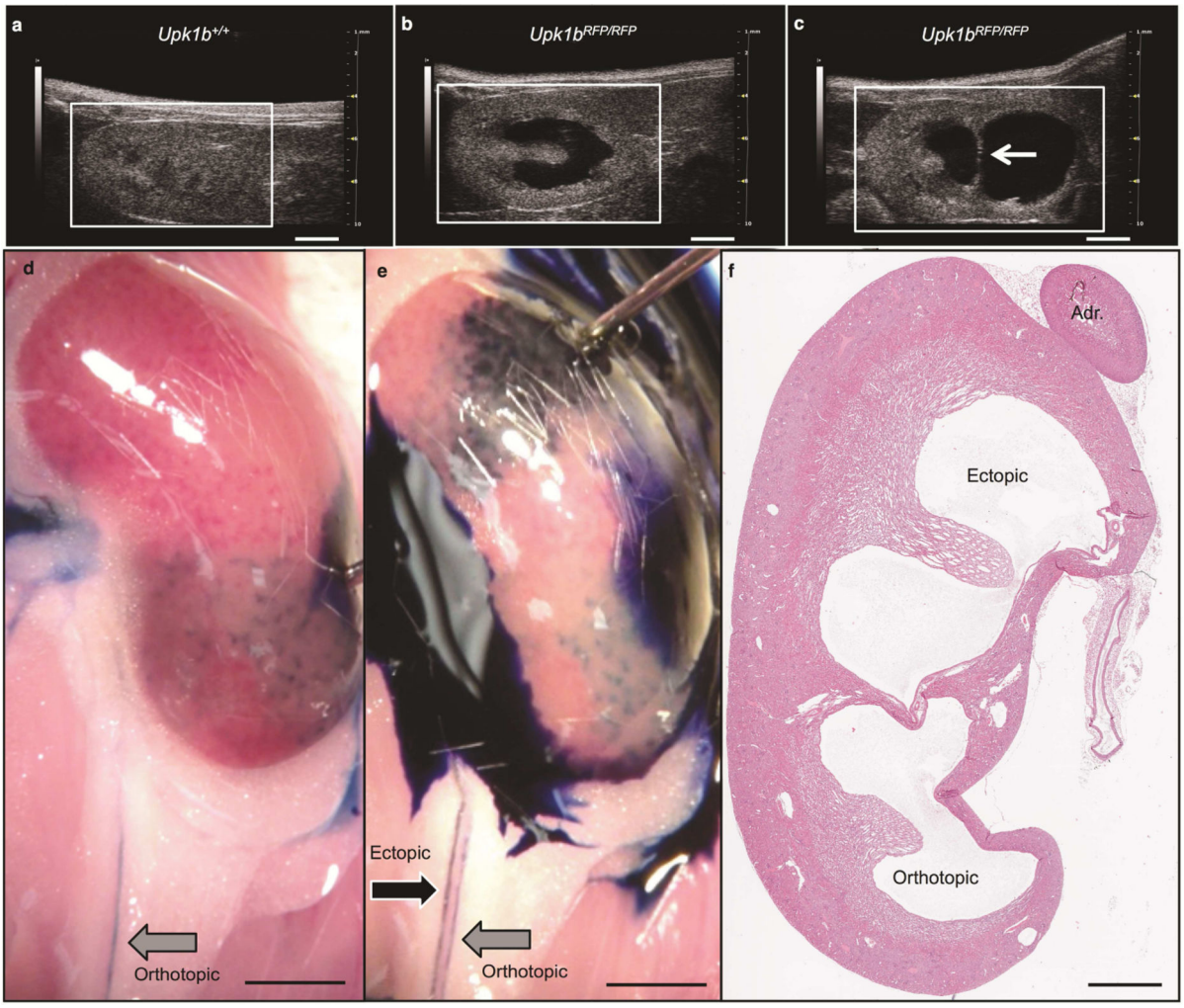

Figure 8. Identification of a Duplicated Collecting System

(A-C) Renal ultrasound was used to evaluate *Upk1b*$^{+/+}$ and *Upk1b*$^{RFP/RFP}$ adult mice to discern (A) normal renal structure, the presence of (B) hydronephrosis, or (C) hydronephrosis and collecting system duplication. White Arrow: Echogenic strip separating two renal pelvises. (D, E) Gross evaluation paired with methylene blue injection directly into the orthotopic (bottom, D) and ectopic (top, E) renal pelvises was used to identify two parallel ureters exiting the kidney. Black Arrow: Ectopic Ureter, Gray Arrow: Orthotopic Ureter. (F) The presence of ectopic and orthotopic pelvises, was analyzed by H&E staining. Adr (Adrenal Gland). Scale bars indicate 2mm, (A-E) 1mm (F).

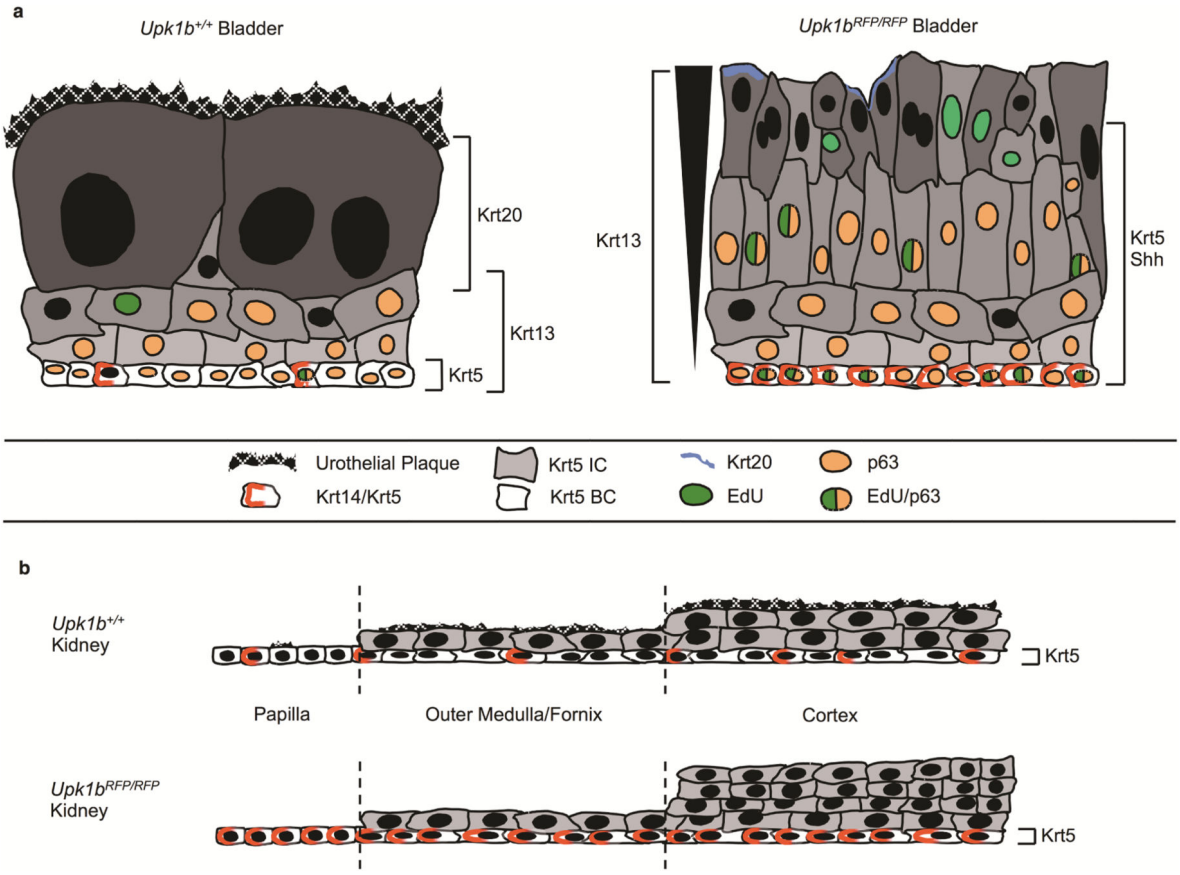

Figure 9. Schematic Depiction of Urothelial Organization

(A) Bladder urothelium in *Upk1b*$^{+/+}$ and (B) *Upk1b*$^{RFP/RFP}$ mice. (C) Renal urothelium is depicted in the papilla, medulla/fornix, and cortex of *Upk1b*$^{+/+}$ and (D) *Upk1b*$^{RFP/RFP}$ mice. The differential expression of urothelial proteins is displayed for Krt5, Krt14/Krt5, Krt13, Krt20, p63, Shh, in addition to proliferation as indicated by EdU, and the presence of an Urothelial Plaque.

Table I

Histopathology Scoring Criteria

Score	Criteria - Urothelial Thickening and Vacuolation
0	***Within Normal Limits***
	- mucosa averages 2-3 cells thick, urothelial cells have roughened apical surfaces
	- no large vacuoles or apoptotic cells, and rare epithelial cell nuclei in the superficial urothelium
1	***Minimal***
	- mucosa averages 3-5 cells thick, urothelial cells generally have smooth apical surfaces
	- rare (1-2) large vacuoles or apoptotic cells but occasional epithelial cell nuclei in the superficial urothelium
2	***Mild***
	- mucosa averages 4-7 cells thick, urothelial cells have smooth apical surfaces
	- occasional (3-5) large vacuoles or apoptotic cells but many epithelial cell nuclei forming a discontinuous layer in the superficial urothelium
3	***Moderate***
	- mucosa averages 7-10 cells thick, urothelial cells have smooth apical surfaces
	- some (6-10) large vacuoles or apoptotic cells with many epithelial cell nuclei forming a nearly continuous layer in the superficial urothelium
4	***Marked***
	- mucosa averages 12 or more cells thick, urothelial cells have smooth apical surfaces
	- many (12+) large vacuoles or apoptotic cells with many epithelial cell nuclei forming a nearly continuous layer in the superficial urothelium

Table II

Urinary Bladder Score - Extent of Urothelial Thickening and Variolation

Genotype	Normal (0)	Minimal (1)	Mild (2)	Moderate (3)	Marked (4)
Upk1b$^{+/+}$ *#1*	x				
Upk1b$^{+/+}$ *#2*	x				
Upk1b$^{+/+}$ *#3*	x				
Upk1b$^{RFP/+}$ *#1*	x				
Upk1b$^{RFP/+}$ *#2*	x				
Upk1b$^{RFP/+}$ *#3*	x				
Upk1b$^{RFP/+}$ *#4*	x				
Upk1b$^{RFP/RFP}$ *#1*			x		
Upk1b$^{RFP/RFP}$ *#2*				x	
Upk1b$^{RFP/RFP}$ *#3*				x	
Upk1b$^{RFP/RFP}$ *#4*					x

Table III

Macroscopic Pathology Scoring Criteria

Score	Criteria - Degree of Hydronephrosis (H&E stained slide)
0	***Within Normal Limits*** - no dilation of the renal pelvis
1	***Minimal*** - pelvis visibly dilated, occupying less than 15% of the kidney width at the hilus
2	***Mild*** - pelvis visibly dilated, occupying 20% to 40% of the kidney width at the hilus
3	***Moderate*** - pelvis visibly dilated, occupying 45% to 70% of the kidney width at the hilus
4	***Marked*** - pelvis visibly dilated, occupying more than 75% of the kidney width at the hilus

Table IV

Kidney Score - Extent of Hydronephrosis

Genotype	Normal (0)	Minimal (1)	Mild (2)	Moderate (3)	Marked (4)
Upk1b$^{+/+}$ *#1*	x				
Upk1b$^{+/+}$ *#2*	x				
Upk1b$^{+/+}$ *#3*	x				
Upk1b$^{RFP/+}$ *#1*	x				
Upk1b$^{RFP/+}$ *#2*	x				
Upk1b$^{RFP/+}$ *#3*	x				
Upk1b$^{RFP/RFP}$ *#1*				x	
Upk1b$^{RFP/RFP}$ *#2*				x	
Upk1b$^{RFP/RFP}$ *#3*					x
Upk1b$^{RFP/RFP}$ *#4*					x
Upk1b$^{RFP/RFP}$ *#5*					x